A Novel UAV Electric Propulsion Testbed for Diagnostics and Prognostics

George E. Gorospe Jr
Chetan S. Kulkarni
SGT Inc., NASA Ames Research Center
Moffett Field, California 95035
george.e.gorospe@nasa.gov
chetan.s.kulkarni@nasa.gov

***Abstract*—This paper presents a novel hardware-in-the-loop (HIL) testbed for systems level diagnostics and prognostics of an electric propulsion system used in UAVs (unmanned aerial vehicle). Referencing the all electric, Edge 540T aircraft used in science and research by NASA Langley Flight Research Center, the HIL testbed includes an identical propulsion system, consisting of motors, speed controllers and batteries. Isolated under a controlled laboratory environment, the propulsion system has been instrumented for advanced diagnostics and prognostics. To produce flight like loading on the system a slave motor is coupled to the motor under test (MUT) and provides variable mechanical resistance, and the capability of introducing nondestructive mechanical wear-like frictional loads on the system. This testbed enables the verification of mathematical models of each component of the propulsion system, the repeatable generation of flight-like loads on the system for fault analysis, test-to-failure scenarios, and the development of advanced system level diagnostics and prognostics methods. The capabilities of the testbed are extended through the integration of a LabVIEW-based client for the Live Virtual Constructive Distributed Environment (LVC-DC) Gateway which enables both the publishing of generated data for remotely located observers and prognosers and the synchronization the testbed propulsion system with vehicles in the air. The developed HIL testbed gives researchers easy access to a scientifically relevant portion of the aircraft without the overhead and dangers encountered during actual flight.**

I. Introduction

Hardware-in-the-loop (HIL) testing of propulsion systems for electric aircraft enable the in-depth investigation of complex propulsion system behavior in a controlled environment. Within the testbed, a propulsion system can be instrumented beyond the requirements or capabilities of flight systems, providing additional insight unavailable otherwise. Furthermore, automated testing of the propulsion system allows for multiple identical operations that can expose natural variance or precursors of component degradation. The use of actual flight data and the generation of flight like loads on the system under test further enhances the applicability of the data created through such testing. HIL testbeds limit system risk, personnel overhead, and overall cost while generating real value as an effective tool for performance and behavior characterization of these critical systems.

The use of HIL testbeds is especially advantageous for the development of diagnostic and prognostic methodologies. HIL testbeds benefit model verification, fault modeling, and as run-to-failure data for a particular system or component may not exist or may be impacted by the excessive system noise or a naturally variable environment, HIL testbeds offer a low risk opportunity to create this valuable data.

For propulsion systems, the controlled environment of a testbed temporarily removes some system variability enabling the extraction of desired features from the collected data. In this environment, the full system may be evaluated at a variety of points within its full operating range; the performance data generated from these sweeping tests can be used for the refinement and verification of mathematical models. Occasionally, HIL testbeds can also be used for the destructive or non-destructive injection of faults within the system or component under test, this is particularly valuable for critical systems such as propulsion systems where some faults cannot be injected during fielded operation. In these cases, data from operation under faulted conditions or during the propagation of a fault can be used for verification of fault models.

With the component model and ancillary fault modeling complete, a prototype prognostic algorithm can be developed and verified though the unique capability of the HIL testbed to perform multiple run-to-failure scenarios. In these scenarios prognostic algorithm performance can be measured by evaluating the predicted and actual remaining useful life of the system. Additionally, the use of HIL testbeds enables multiple tests of the integrated system under varied conditions to evaluate the robustness of the algorithm to load and noise variance.

When prognostics technology is applied to individual components or the full propulsion system itself, it can be used for the determination of the system health state and the prediction of critical events, such as the the end of life (EOL) or the crossing of a significant performance threshold. This information is valuable to operators who can make more informed maintenance, operational, or mission-level decisions. Autonomous systems can also make use of this information for health state aware action or prognostic decision making [1].

This paper presents the design and initial results from the development of a new electric propulsion system testbed for diagnostics and prognostics. The testbed was utilized in the development of new models, and the verification of

prognostic algorithms. Additionally, the testbed was developed with the capability to publish and subscribe to data from the Live Virtual Connected Development Environment (LVC-DE) through the LVCgateway.

The structure of the paper is as follows. Section II introduces the reference aircraft and the components of the propulsion system. Section III discusses the overall design of the prognostics testbed and describes the faults injected in the system. Section IV briefly describes the integration with prognostics algorithms. Section V discusses the experiments conducted with the testbed and some illustrative prognostics results. The paper ends with a brief discussion and conclusions in Section VI.

II. Unit Under Test

Electric propulsion systems for small UAVs offer desirable features such as high efficiency, low vibration and heat byproducts, and no gaseous exhaust. The electric propulsion system testbed, referred to as the "Iron Edge" testbed, was built referencing the all electric, Edge 540T aircraft used in science and research by NASA Langley Flight Research Center [2] . The Iron Edge testbed features an identical propulsion system, consisting of brushless direct current (BLDC) motors, electronic speed controllers (ESCs) and Lithium-polymer (LiPo) batteries. Figure 1 shows the overall layout of the system.

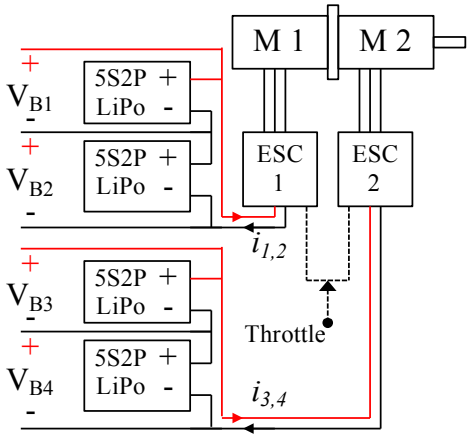

Fig. 1. Edge 540T Propulsion System Diagram

The Edge 540T aircraft is a commercially available 33% scale model of the Zivko Edge 540T. Pictured in figure 1, the Edge 540T is 96 inches long with a 100 inch wing span (2.5 m x 2.5 m) and an approximate weight of 55 lbs (25 kg). The aircraft is used for technology research and development missions features instrumentation for automated operation, structural fault diagnosis, and power system health monitoring. Flight data captured by the onboard data acquisition system includes, motor RPM, motor temperature, accelerometer data, battery voltage and current draw, and GPS location.

The motor system used by the Edge 540T and included in the testbed is a pair of mechanically coupled AXI Gold 5330/20 double outrunner BLDC motor powered by individual

Fig. 2. Edge 540T in Flight

ESCs and battery banks. This system replaces the original internal combustion engine used by the Edge 540T. Each motor in the motor system has an internal resistance of 0.045 ohms and is well suited for voltages between 42 VDC and 32 VDC. A pair of Jeti Advance 90 Pro Opto programmable ESCs provide external electronic commutation for each motor in the motor system. These ESCs can provide a sustained current rating of 90 amps and a supply voltage range of 12 - 42 VDC. The ESCs require a supply voltage between 14-30 VDC and a nominal 50 Hz PWM servo input signal.

Dual LiPo battery banks provide the direct current for the ESCs. Each battery bank consists of two LiPo batteries rated at 7800 mAh with a 50 C maximum burst discharge. Each battery is made up of 5 individual cells in parallel; the fully charged open-circuit voltage of each battery is 21 VDC or 4.2 VDC per cell.

Model development for the motor, ESCs, and batteries can be found in previous work [3] [4]. The individual models have been coupled together to provide propulsion system level insight and serve as the basis for new model-based prognostic methodologies.

III. Prognostic Testbed Design

The challenges associated with the design of the Iron Edge electric propulsion system testbed for diagnostics and prognostics include a requirement to recreate the flight system control interface, motivation to reproduce realistic flight-like loads on the system under test, and the unique task of creating realistic, non-destructive, controllable faults within the system. The bench-top nature of the testbed enables the use of capable data acquisition and control (DAQ) equipment and powerful desktop workstations to address these challenges. Within the testbed, the DAQ and workstation is used for signal generation, monitoring, user interface, control, networking, and data storage. To ensure safe operation, the testbed was built inside of a fire-proof metal junction box equipped with emergency power cutoff switches. Ultimately, the final system must be able to simulate flight-like operations, inject realistic faults

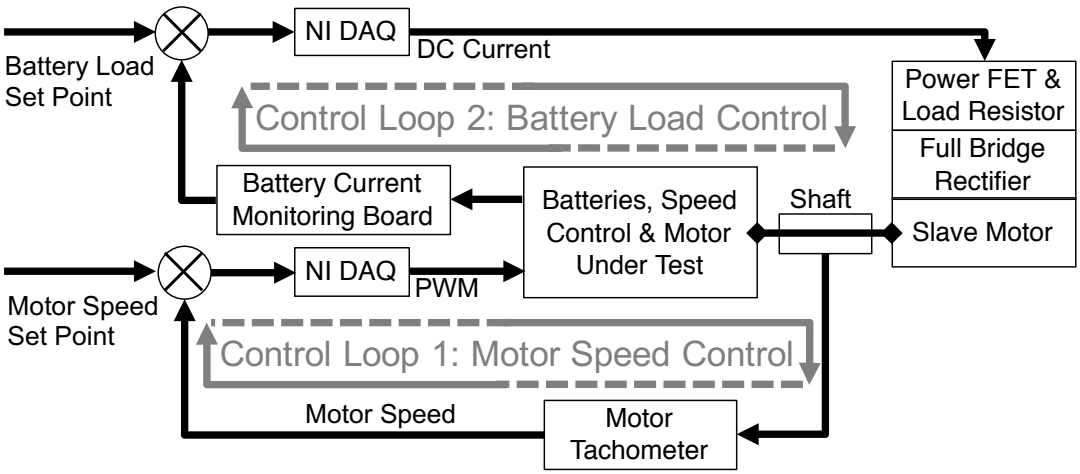

Fig. 3. Control Loops for Motor Speed Control and Battery Loading

within the system under test, and demonstrate diagnostic and prognostic technologies such as fault detection and isolation, state of charge prediction and the estimation of remaining useful life.

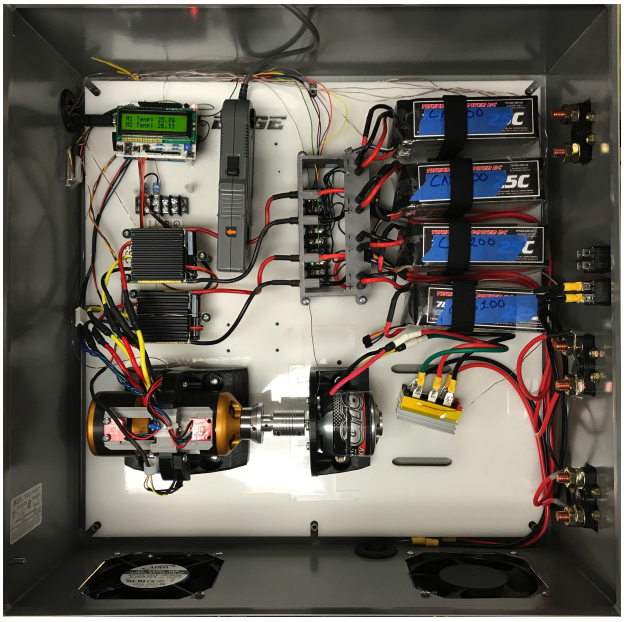

Fig. 4. Iron Edge Testbed Layout

A. Instrumentation and Control

Given the components of the reference propulsion system, a new LabVIEW-based application was created to produce control input for the propulsion system and acquire sensor information from the testbed. The LabVIEW application also manages higher level control of the system including closed-loop the speed control of motor and closed loop control of the mechanical load applied the propulsion system. The user interface for the application is shown below.

The primary control input for the propulsion system is the throttle, a pulse width modulated (PWM) signal operating at 50 Hz, that directly controls the motor speed. This signal, generated by the National Instruments cDAQ, is fed to each ESC, and drives the switching frequency of the half-bridge circuits applying current to the BLDC motor windings. The

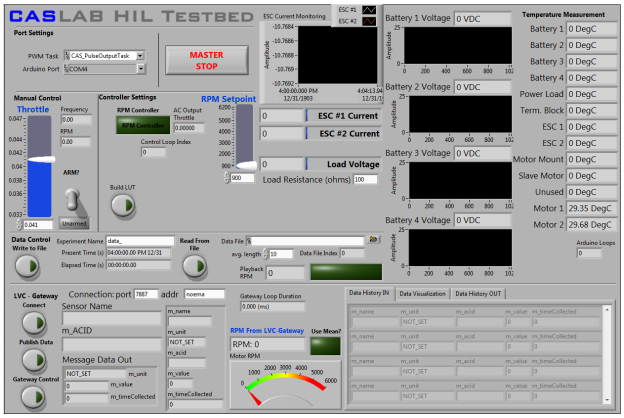

Fig. 5. Testbed User Interface

testbed features instrumentation similar to the flight system, battery voltage and current measurement as well as temperature measurement for the batteries and motor. The testbed also has additional sensors for advanced system diagnostics. The ESCs are each instrumented for temperature at the junction between their circuit board and the heat sink. Motor temperature is measured at the motor mounting plate via thermocouple and at the surface of each of the rotating stator covers via IR thermopile. The motor speed is measured directly at the shaft with an IR emitter/receptor. Additionally, the slave motor mounting plate is instrumented for temperature sensing.

Higher level control logic such as motor speed control and control of the applied mechanical load, enables testbed to replay previously recorded flight data, achieve flight like loading on the propulsion system, and simulate faults within

the system. The testbed achieves higher level control logic through the use of two control loops. The first loop, the motor control loop achieves the motor speed set point through throttle control and monitoring of the motor tachometer. The second control loop, achieves the desired battery current draw load set point through the actuation of a power FET controlling the resistance of the rectified current produced by the slave motor and monitoring the produced current draw from the batteries. In this configuration, the slave motor is mechanically driven by the MUT and behaves like a generator. producing current on all three of it windings. This current is rectified and the resulting direct current is managed by a power FET and power load. Both control loops are pictured in Fig. 3.

B. Network Capability

The HIL testbed features additional networking functionality to connect to a new distributed testbed called the Prognostic Virtual Laboratory. The Prognostics Virtual Laboratory is a modular infrastructure for distributed aircraft prognostics experimentation [5]. When connected to the virtual lab infrastructure via the LVC Gateway, a message exchange server, the HIL testbed can both publish sensor information and subscribe to messages originating on other connected modules, such as fielded aircraft, virtual aircraft, or agents playing back previously recorded flight data. Additionally, any connected modules may also subscribe to the sensor messages originating at the HIL testbed. Server-based prognosers, software tools created to apply the latest model-based prognostic methods to incoming sensor information, can produce prognostic results through the remote monitoring of sensor information from the HIL testbed. The addition of network functionality and the integration of the testbed within the Prognostics Virtual Laboratory extends test capabilities and creates new opportunities for connected experimentation.

C. Simulated Motor Faults

The controlled injection of a non-destructive fault representative of motor wear is achieved through the application of variable load with a slave motor. The slave motor is mechanically coupled to the MUT and produces a programmatically controlled rotational resistance. The increased rotational resistance is intended to simulate increased rotational friction or wear in the windings of the BLDC motor. The nature of this system enables the creation of both static or dynamic fault conditions.

IV. Diagnostic and Prognostic Approach

The problem presented in this work is divided in two parts, a system level approach for diagnosis and prognostics for RUL estimation as shown in Fig. 6. In this framework a system level fault detection and isolation approach is implemented. Once the fault is isolated, prognostics framework is applied to determine the current health state of the system/ subsystem the future health performance until the RUL is reached. Earlier work studied approaches for fault detection [6] and prognostics [3], [7], [8] at the component level while in this work we discuss implementing a system/subsystem level approach.

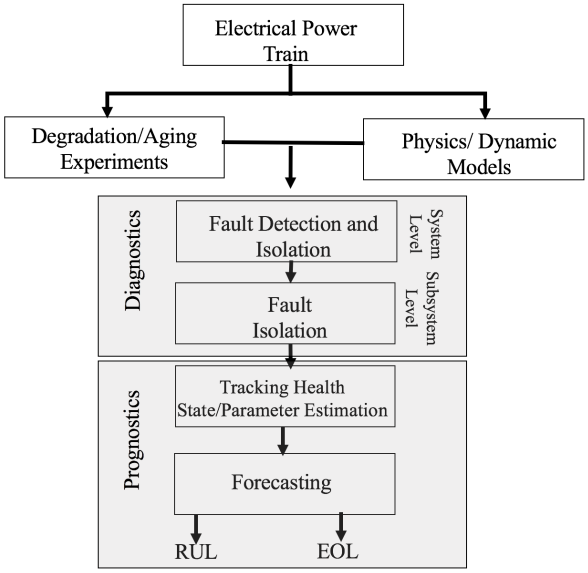

Fig. 6. Research Approach

The diagnosis architecture includes an observer that tracks the continuous-behavior and discontinuous-mode changes in the system. When the output data from the observer deviates significantly from the seen behavior, the fault detector is triggered which then runs the fault-isolation scheme. As per the International Federation of Automatic Control Technical Committee a fault is defined as "an unpermitted deviation of at least one characteristic property or parameter of the system from acceptable, usual, or standard conditions" [9].

In the model-based prognostics architecture [10], [11], there are two problems to be solved as shown in Fig.7. First to solve is the *estimation* problem, which determines a joint state-parameter estimate $p(\mathbf{x}(k), \theta(k)|\mathbf{Y}_{k_0}^{k_P})$ based on the history of observations up to time k, denoted as $\mathbf{Y}_{k_0}^{k}$, and second is the *prediction* problem, which determines at prediction time k_P, using $p(\mathbf{x}(k), \theta(k)|\mathbf{Y}_{k_0}^{k_P})$, $p(\mathbf{U}_{k_P})$, $p(\mathbf{V}_{k_P})$, and $p(\Theta_{k_P})$, the probability distribution $p(k_E(k_P)|\mathbf{Y}_{k_0}^{k_P})$. Here, $\mathbf{U}_{k_P}$ denotes the future system inputs from k_P on, $\mathbf{V}_{k_P}$ denotes the future process noise values from k_P on, and Θ_{k_P} denotes the future unknown parameter values from k_P on.

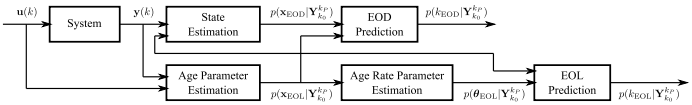

Fig. 7. Research Approach for Battery Example

V. Experimental Results

In this section results and analysis from the experiments are discussed. The following experiments were conducted to implement the developed approach. The first experiment involved testing with both nominal and degraded ESCs under constant loading conditions. The goal of this experiment was to observe performance differences between both the ESCs.

A. Fault scenario: Degraded ESCs

Data collected during actual flights of the Edge 540, discussed previously in section II, is here used to produce flight-like command of the propulsion system testbed. From this data, rpm values were used to simulate flight of the EDGE 540 and the demands on the propulsion system. In the baseline for the first experiment, both the ESCs, as seen from schematic diagram of Fig. 1, are healthy and operating normally. In the second experiment one of the ESCs was replaced with an degraded ESC and operation of both the ESCs was observed.

Voltage and current data from experiment 1 are shown in Fig. 8 and Fig. 9, and experiment 2 plots for degraded ESC operation are shown in Fig. 10 and Fig. 11.

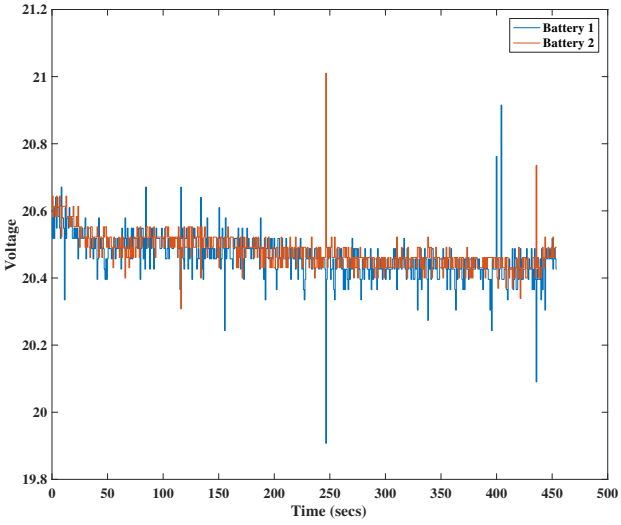

Fig. 8. Voltage profiles of both batteries for New ESC Operation

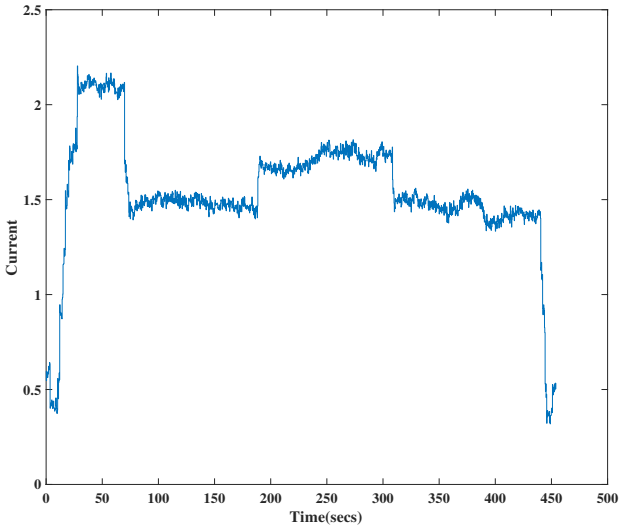

Fig. 9. Current profile for New ESC Operation

Plot in Fig. 12 shows temperature rise for both the nominal and degraded ESC over its operating range. From the plots it is

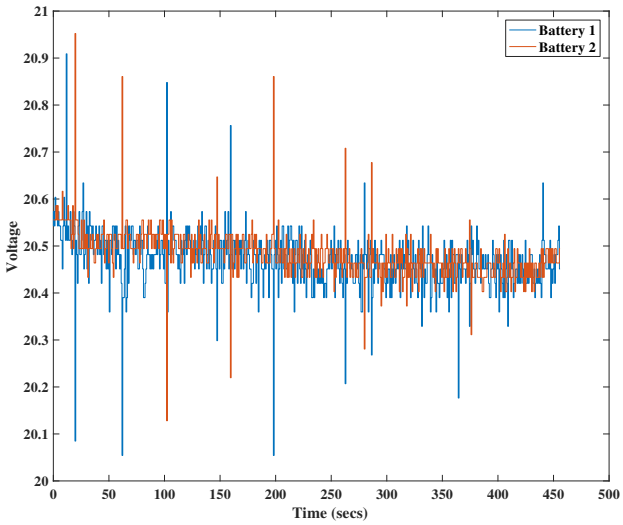

Fig. 10. Voltage profiles of both batteries for Degraded ESC Operation

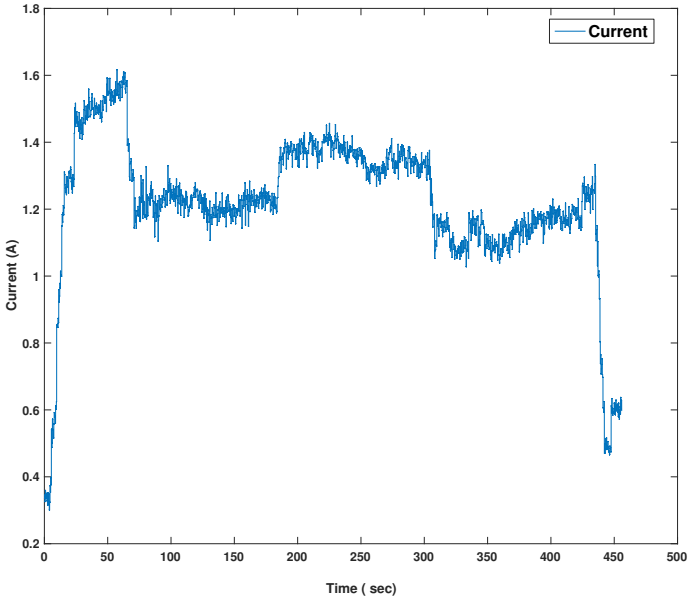

Fig. 11. Current profile for Degraded ESC Operation

observed that the degraded ESC temperature was significantly higher than the nominally operating ESC.

B. Fault Isolation

For this initial demonstration of an electric propulsion system diagnostic approach, we implemented a basic rule-based fault detection and isolation method. Later, this approach can be replaced by any other FDI method as a part of future research. To perform fault isolation, we focused mainly on the current drawn from the batteries and the increase in respective ESC and motor temperature. From the above plots It is observed that degraded ESC draws more current as compared to an healthy ESC. In addition there is a significant difference in the temperature residuals of healthy and degraded ESCs. Table I shows a matrix for isolating each of the faults in the

TABLE I
RESIDUAL TRIGGER MATRIX FOR FAULT ISOLATION

System	ESC1	ESC2	M1	M2	Battery-I	Battery-V
ESC1	✓	✗	✗	✗	✗	✗
ESC2	✗	✓	✗	✗	✗	✗
M1	✓	✓	✓	✗	✓	✗
M2	✓	✓	✗	✓	✓	✗
Battery-I	✓	✓	✓	✓	✓	✗
Battery-V	✓	✓	✗	✗	✓	✓
Fault Detected	✓	✓	✓	✓	✓	✓

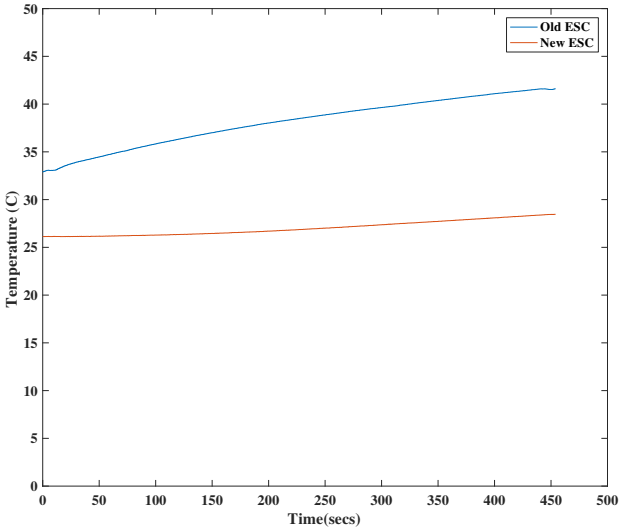

Fig. 12. Variation in Temperature between New and Degraded ESC's

system. ESC1 and ESC2 are respective temperatures of the ESCs. Similarly, M1 and M2 are the respective temperatures of the motors. Battery-I and Battery-V are the currents and voltage residuals from the batteries.

VI. CONCLUSION

In this paper we have described a new UAV electric propulsion testbed for the development of diagnostics and prognostics technology. This testbed was used for the continued refinement of mathematical models in the context of model-based prognostics and the development of propulsion system wide diagnostic techniques. This initial work completed with the testbed is a key step to the deployment of such technologies onboard flight vehicles.

Initial results suggest that the data produced by the testbed can be used for implementing a system level FDI and Prognostics framework. Future work will include the long term tracking of the battery health state and the end-of-life estimation for each battery in the the system, refinement of the system level diagnostics capabilities, and integration of the actual flight DAQ system and instrumentation to replace the laboratory grade DAQ equipment currently in use.

REFERENCES

[1] E. Balaban, S. Narasimhan, M. Daigle, I. Roychoudhury, A. Sweet, C. Bond, and G. Gorospe, "Development of a mobile robot test platform and methods for validation of prognostics-enabled decision making algorithms," *International Journal of Prognostics and Health Management*, vol. 4, no. 1, 2013.

[2] B. Bole, C. A. Teubert, Q. Cuong Chi, E. Hogge, S. Vazquez, K. Goebel, and G. Vachtsevanos, "Silhil replication of electric aircraft powertrain dynamics and inner-loop control for v&v of system health management routines," 2013.

[3] M. J. Daigle and C. S. Kulkarni, "Electrochemistry-based battery modeling for prognostics," *Annual Conference of the Prognostics and Health Management Society*, pp. 249–261, October 2013.

[4] G. E. Gorospe, C. S. Kulkarni, E. Hogge, A. Hsu, and N. Ownby, "A study of the degradation of electronic speed controllers for brushless dc motors," *Annual Conference of the Prognostics and Health Management Society Asia Pacific*, July 2017.

[5] C. Kulkarni, G. Gorospe, C. Teubert, C. Quach, K. Darafsheh, and E. Hogge, "Application of prognostics methodology to virtual laboratory for future aviation and airspace research application of prognostics methodology to virtual laboratory for future aviation and airspace research application of prognostics methodology to virtual laboratory for future aviation and airspace research," in *AIAA Modeling and Simulation Technologies Conference*, AIAA, Ed., January 2017.

[6] S. Poll and et. al., "Advanced diagnostics and prognostics testbed," in *18th International Workshop on Principles of Diagnosis*, May 2007.

[7] J. Celaya, C. Kulkarni, K. Goebel, and G. Biswas, "Prognostic studies and physics of failure modeling under high electrical stress for electrolytic capacitors," *International Journal of Prognostics and Health Management*, vol. 3(2), pp. 1 – 18, 2012.

[8] J. R. Celaya, A. Saxena, C. S. Kulkarni, S. Saha, K. G. J. R. Celaya, A. Saxena, C. S. Kulkarni, S. Saha, and K. Goebel, "Prognostics approach for power mosfet under thermal-stress aging," in *Proceedings Annual Reliability and Maintainability Symposium*, IEEE, Ed. IEEE, 2012.

[9] S. Narasimhan and G. Biswas, "Model-based diagnosis of hybrid systems," in *IEEE TRANSACTIONS ON SYSTEMS, MAN, AND CYBERNETICS—PART A: SYSTEMS AND HUMANS*, vol. 37, no. 3, May 1997.

[10] M. Daigle and K. Goebel, "Model-based prognostics with concurrent damage progression processes," *IEEE Transactions on Systems, Man, and Cybernetics: Systems*, vol. 43, no. 4, pp. 535–546, May 2013.

[11] M. Daigle and S. Sankararaman, "Advanced methods for determining prediction uncertainty in model-based prognostics with application to planetary rovers," in *Annual Conference of the Prognostics and Health Management Society 2013*, October 2013, pp. 262–274.